



**National  
Oceanography Centre**  
NATURAL ENVIRONMENT RESEARCH COUNCIL

## **National Oceanography Centre**

### **Research & Consultancy Report No. 71**

Sensitivity of AMM15-surge to varying tidal boundary  
conditions and bottom friction coefficients

David Byrne<sup>1</sup>, Kevin Horsburgh<sup>1</sup>, Clare O'Neill<sup>2</sup>

2019

<sup>1</sup> National Oceanography Centre, Liverpool, U.K., L3 5DA

<sup>2</sup> UK Met Office, Exeter, U.K., EX1 3PB

National Oceanography Centre  
Joseph Proudman Building  
Brownlow St Liverpool  
L3 5DA

Email: [dbyrne@noc.ac.uk](mailto:dbyrne@noc.ac.uk)

# Contents

|          |   |           |
|----------|---|-----------|
| <b>1</b> | <b>Introduction</b>                                 | <b>3</b>  |
| <b>2</b> | <b>Outline of Experiments</b>                       | <b>5</b>  |
| 2.1      | Model Setup & Control Experiment . . . . .          | 5         |
| 2.2      | Varying Tidal Boundary Conditions . . . . .         | 5         |
| 2.3      | Varying Bottom Friction Coefficient . . . . .       | 6         |
| 2.4      | Diagnostics and Metrics . . . . .                   | 6         |
| <b>3</b> | <b>Data</b>   | <b>7</b>  |
| 3.1      | Model Output . . . . .                              | 7         |
| 3.2      | Observational Data . . . . .                        | 7         |
| 3.3      | External Model data . . . . .                       | 7         |
| <b>4</b> | <b>Results</b>                                      | <b>8</b>  |
| 4.1      | Comparison of AMM15 (Control Run) to AMM7 . . . . . | 8         |
| 4.2      | Variation of Tidal Boundary Conditions . . . . .    | 11        |
| 4.2.1    | Amplitude and Phase . . . . .                       | 11        |
| 4.2.2    | Tidal Range and High Water Lag . . . . .            | 17        |
| 4.3      | Varying the Bottom Friction Coefficient . . . . .   | 21        |
| 4.3.1    | Amplitude and Phase . . . . .                       | 21        |
| 4.3.2    | Tidal Range and High Water Lag . . . . .            | 27        |
| <b>5</b> | <b>Summary and Recommendations</b>                  | <b>32</b> |

# 1 Introduction

Operational storm surge forecasting at the Met Office is undergoing transition from the model code developed by the National Oceanography Centre (NOC) to new configurations based on a depth-averaged configuration of the NEMO ocean model (Madec et al., 1998; Madec et al., 2014). The legacy configurations of CS3X (e.g. Horsburgh et al., 2008; Flowerdew et al., 2010) will continue to run in deterministic and ensemble modes during 2019/2020 but will be retired shortly thereafter once the NEMO suite can supply all operational products to the UK stakeholders.

The NEMO-surge tidal model developed by Furner et al. (2016) was shown to have tidal prediction accuracy that was at least as good as the existing CS3X model, at a similar spatial resolution. This report describes a joint research project between the NOC and the Met Office to investigate the improvement of tidal predictive accuracy with increased model resolution. A long-term aspiration for operational forecasting is to use a consistent model product for total water level, rather than the current practice of adding model-derived storm surge to harmonically predicted tides. Since the tidal component is a significant part of total water levels for most UK locations then there is a clear need to optimise tidal performance in the NEMO model.

The configuration of the NEMO tide-surge model used for these results used an existing domain at approximately 1.5km horizontal resolution (called AMM15). We present two sets of sensitivity experiments where for simplicity there is no atmospheric forcing (i.e. the model was run in tide-only mode). The first of these compared three different options for lateral tidal boundary conditions (with varying numbers of tidal constituents). The performance of the AMM15 model was compared with the operational CS3X model, and also with an intermediate 7km resolution model (AMM7), by evaluating tidal parameters against those observed at 41 UK tide gauges and quality controlled by the British Oceanographic Data Centre (BODC). For the largest (and most important in terms of water level) tidal constituents the best performance was obtained with lateral boundary forcing from 15 satellite-derived constituents (the TPX09 tidal dataset). For the semidiurnal (M2 and S2) constituents, the 1.5km model forced by TPX09 gave better results than either CS3X or the 7km model. Tidal phase accuracy was mostly improved, compared to the coarser resolution models, for five of the six largest constituents (but not M2). Performance with forcing from the FES2014 dataset was similar overall. Both gave significantly better results than the boundary conditions derived from a larger numerical model (NEA), despite this offering more constituents.

We also examined the modelled tidal response to three different values of the coefficient of bottom friction, all lower than in the control run. In all cases, lowering the value of the coefficient resulted in increased errors for both tidal amplitude and phase.

In summary, we found that overall the finer resolution 1.5km AMM15 tide-surge model delivers an improved performance over the coarser CS3X or AMM7 models. Notable improvements of up to 20cm in amplitude were obtained in the Severn Estuary. Our results suggest that the optimal configuration would be to use either TPX09 or FES2014 lateral boundary conditions as tidal input, and a value of 0.0024 for the coefficient of bottom friction. It should be noted that the higher resolution model requires

significantly more computational time, which should be borne in mind when assessing the operational benefit (particularly when ensembles will be run).

## 2 Outline of Experiments

Two sets of experiments have been performed for this report. The first evaluates model sensitivity to a choice of three tidal boundary datasets with varying numbers of tidal constituents. The second examines the sensitivity to a varying bottom friction coefficient (discussed more in Section-2.3).

Summaries of each model run and their abbreviations are shown in Table-1

| Model Abbrev. | Description   |
|---------------|---|
| CTRL (TPXO)   | Control experiment for comparison. Uses 15 tidal constituents from TPXO9 dataset and a bottom friction coefficient of $C_B = 0.0024$ with quadratic parameterisation. |
| FES           | Uses 31 constituents from FES2014 data. Same bottom friction as control.  |
| NEA           | Uses 26 constituents from NEA dataset. Same bottom friction as control  |
| BF22          | Uses same tidal forcing as control with a modified bottom friction coefficient of $C_B = 0.0022$ .  |
| BF20          | Uses same tidal forcing as control with a modified bottom friction coefficient of $C_B = 0.0020$ .  |
| BF18          | Uses same tidal forcing as control with a modified bottom friction coefficient of $C_B = 0.0018$ .  |

Table 1: Abbreviations of model runs performed for this report.

### 2.1 Model Setup & Control Experiment

The results in this report have been generated using NEMO-surge; a 2D, barotropic version of NEMO [2]. The specific configuration used has been on a 2D version of the domain used for the AMM15 configuration (Atlantic Margin Model, 1.5km) [1]. See [3] for more information on how NEMO was adapted to work in a 2-dimensional barotropic state.

Each model run in this report is performed for 44 months, following 8 weeks of spinup. A longer spinup (up to a year) might have been more beneficial but 8 weeks was chosen to be sufficient for most constituents, computing resources considered.

A control experiment has been performed in order to have a baseline for all the experiments in this report to be compared to. The control experiment uses 15 constituents from the TPXO9 dataset. A bottom friction coefficient of 0.0024 is used.

### 2.2 Varying Tidal Boundary Conditions

Two tidal datasets (additional to the control) are considered for generating tides at the models lateral boundaries:

1. **FES2014**: 31 constituents used. Generated using a combination of altimetry and a spectral model [4, 5].
2. **NEA**: 26 constituents used. Generated using a large-domain tide model and used operationally with CS3 and CS3X [3].

Both datasets contain more constituents than the TPXO9 data used for the control experiment. There is overlap between each dataset in terms of the constituents included, but also unique constituents in each.

Each dataset is cropped appropriately and interpolated bilinearly onto the model grid. Datasets are manipulated and given to NEMO in complex form, i.e. with  $z_1$  and  $z_2$  values.

### 2.3 Varying Bottom Friction Coefficient

Additional to the control experiments value of 0.0024, three values for  $C_B$  are investigated: 0.0022, 0.0020 and 0.0018. All three values are less than the value used in the control and were decided on based on the results in Section-4.2.

### 2.4 Diagnostics and Metrics

The following metrics are used throughout this report for judging model skill:

1. **RMSE**. The root mean squared error.
2. **ME**. The mean error (or bias).
3. **AE**. Absolute error.

The following physical quantities are estimated from model or observed time series:

1. **Tidal Range**: The difference between the height of high water and low water in a given tidal cycle. This has been calculated by identifying all high/low waters in a given time series and differencing them. Where data was missing during a tidal cycle, the whole cycle was rejected.
2. **High Water Lag**: The difference in the timing of high water between the model and observations. This was calculated in a similar fashion to tidal range: by first identifying the locations of high waters. It is important to note that both the observation and model data used is hourly, therefore the error bars are large.

Errors in the amplitude and phase of harmonic constituents as well as in TR and HWL are studied at individual locations and averaged across all locations. Locations used and the source of their data is discussed in Section-3.

## 3 Data

### 3.1 Model Output

Hourly 2-dimensions sea surface height data is saved from NEMO-surge into netcdf format. These files are large therefore time series are extracted at each class A tide gauge location (see next section) using NCO-tools.

Harmonic analysis is also performed using the NEMO model. Six constituents are analysed for and discussed further in the results section of this report.

### 3.2 Observational Data

Observed time series of sea level are used for validation of this report’s experiments. Harmonic constituents are derived by BODC from 19-years of observed data at 41 Class A tide gauge locations around the UK.

Time series from 2014 are also used for estimation of tidal range and high water lag. This data is also obtained from BODC and a all data with a QC flag are removed. For some locations, this meant that there was not sufficient data to a meaningful analysis of tidal range and high water lag, i.e. at Bournemouth, Immingham and Port Ellen.

### 3.3 External Model data

Some statistics from other model runs have been used for comparison purposes in this report. The model runs are a similar, coarser NEMO configuration called AMM7 and CS3X, the current model used operationally by the Met Office. Data from Met Office and [1]. Abbreviations used in this report are shown in Table-2.

| Model Abbrev. | Description   |
|---------------|---|
| AMM7          | NEMO configuration with comparable domain to AMM15. 7km resolution with TPXO9 tidal boundary forcing. [1] |
| CS3X          | Used operationally for storm surge forecasting by the Met Office.   |

Table 2: Abbreviations of model runs performed for other studies (referenced) using for comparison purposes in this report.

## 4 Results

### 4.1 Comparison of AMM15 (Control Run) to AMM7

In this section, amplitudes and phases of four harmonic constituents from the control run (CTRL) and AMM7 are compared. This comparison is done to act as a baseline for the subsequent results in the rest of this report. Figures 1-2 show a comparison of absolute errors in harmonic phase and amplitude between the CTRL AMM15 run and AMM7 at 41 UK locations. These figures show a comparison for the four harmonic constituents: M2, S2, K1 and O1.

For all four constituents, amplitudes are improved (or similar) at all locations for the AMM15 control run compared to AMM7. For M2, improvements are largest in the Severn Estuary, reaching up to 20cm improvement. For S2, improvements are more uniform, with largest improvements at Avonmouth and Dover of up to 10cm. Improvements for K1 and O1 are significantly smaller, which is to be expected as the amplitude of these constituents is also smaller. Improvements are largest for K1 in the North of England and Scotland, and improvement are largest for O1 around the west coast of Scotland and Liverpool Bay.

For phase, there improvements are many locations for all four constituents however the picture is less straightforward. The AMM15 control run performs worse at Port Ellen and Immingham for most constituents. The deterioration at Port Ellen is large for M2 and K1, reaching as much as 30 degrees. Improvements are seen, for example, along the south coast for M2, south and east coasts for S2, Liverpool Bay for K1 and south coast for O1. With the except of Port Ellen and Immingham, where there are worse phases from the AMM15 control run, the differences are generally small (less than 10 degrees).

Overall, the AMM15 control run seems to perform better than AMM7, especially for the larger harmonics M2 and S2. Now the report will move its focus onto examining improvement potential for AMM15 by using different tidal forcing and bottom friction parameters.



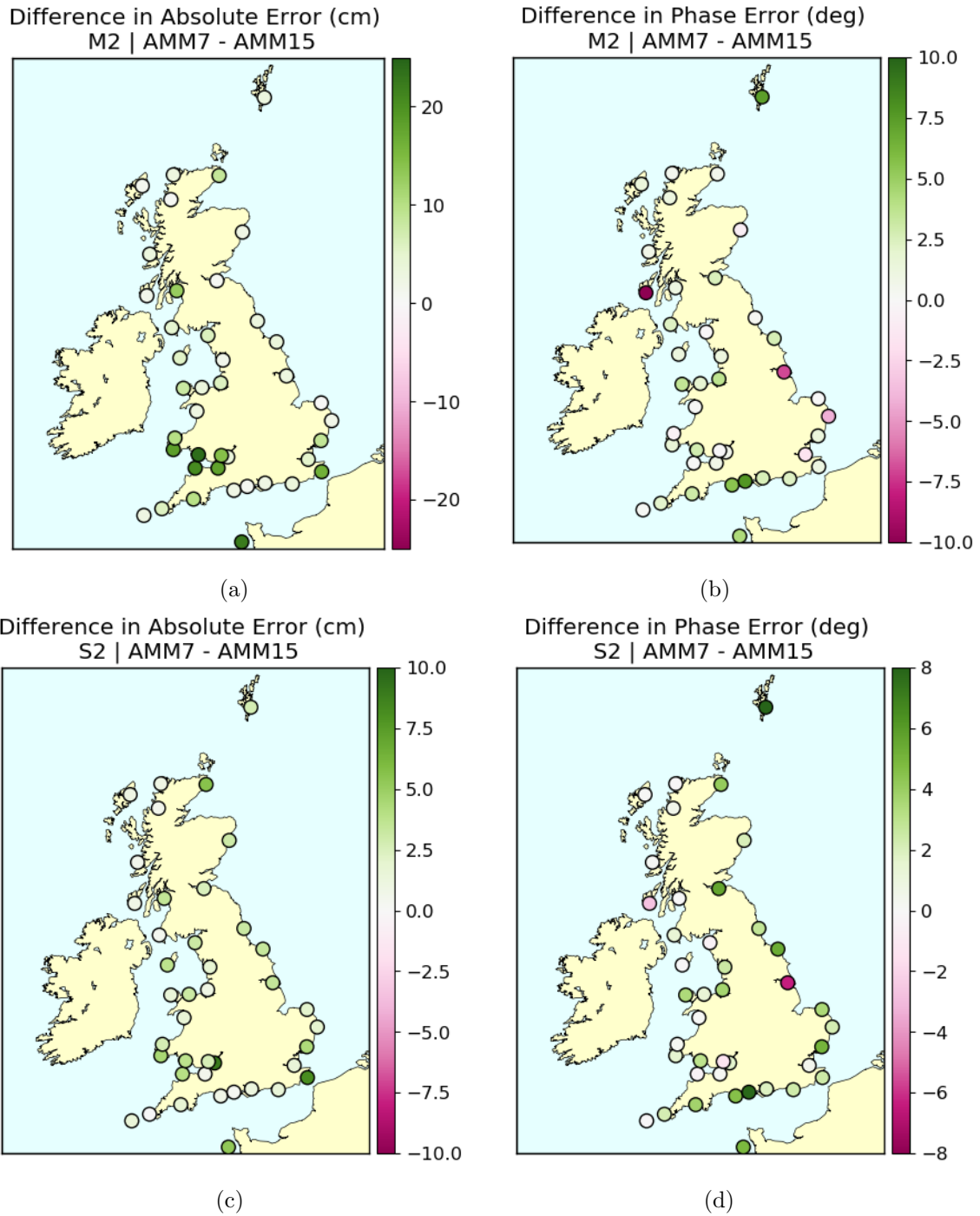


Figure 1: Differences in absolute errors between AMM15 (CTRL run) and AMM7 for amplitude and phase. Left figures are for amplitude and right figures are for phase. Constituents: M2 and S2. Positive indicates AMM15 was better.

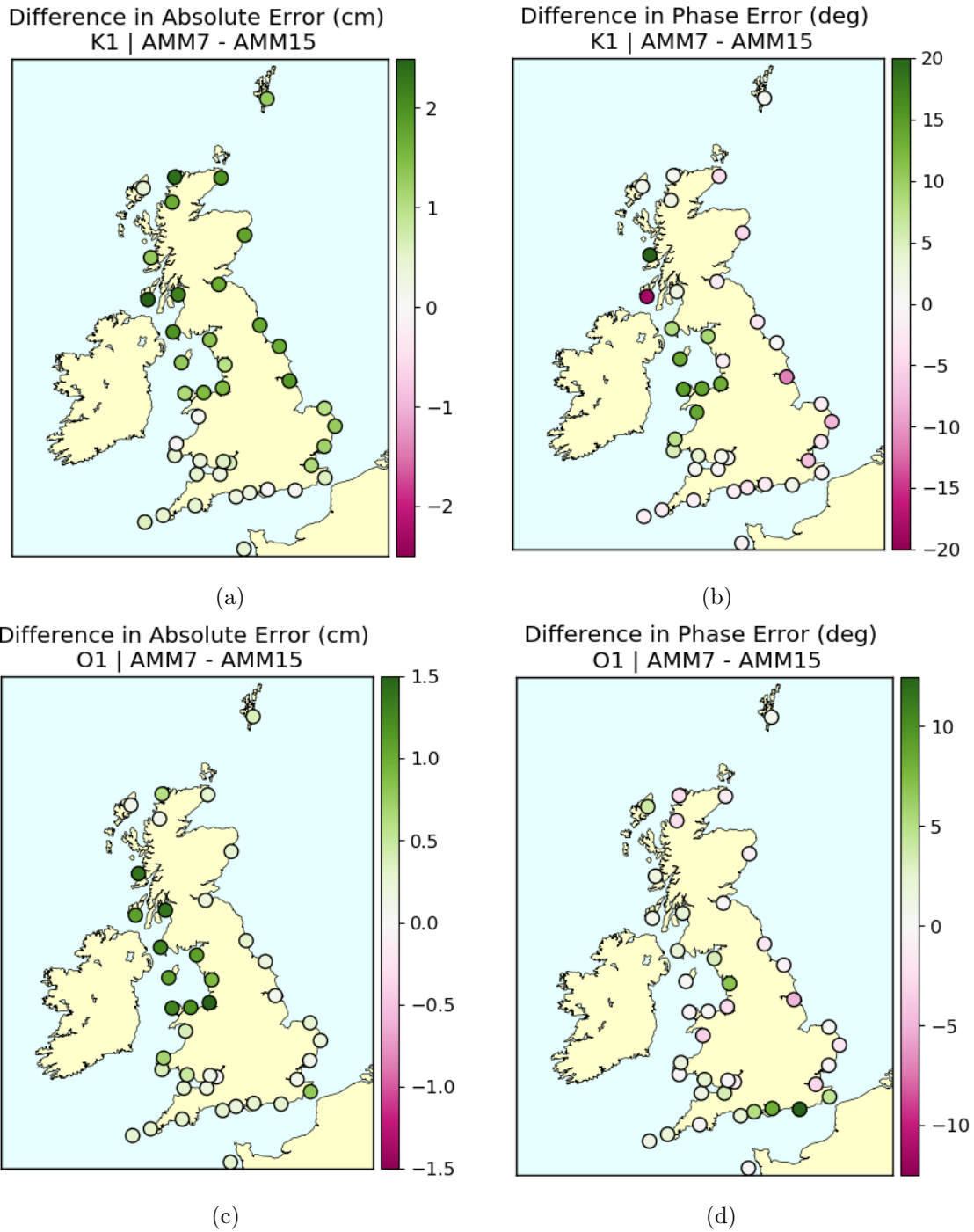


Figure 2: Differences in absolute errors between AMM15 (CTRL run) and AMM7 for amplitude and phase. Left figures are for amplitude and right figures are for phase. Constituents: K1 and O1. Positive indicates AMM15 was better.

## 4.2 Variation of Tidal Boundary Conditions

### 4.2.1 Amplitude and Phase

In this section, the effect of applying different tidal datasets on some of the largest harmonic constituents is examined. Many of the largest constituents are common amongst the three boundary datasets, therefore it is the accuracy of the boundary data and the interactions between constituents being evaluated.

Figure-3 shows the errors in the amplitude of the modelled M2 constituent, which is (generally) the largest and most important constituent. The model performs comparably when using TPXO and FES boundary data, with generally small amplitude errors of no more than 15cm. In both cases, the amplitude is underestimated by the model around the Severn Estuary, much of the English Channel, Straits of Moyle and at Sheerness. Conversely, the model underestimates along most of the East coast, northern Scotland and around Liverpool Bay. When using NEA boundary forcing, the model underestimates the M2 amplitude almost everywhere. Larger errors are seen down the East coast, with magnitudes of up to 30cm being approached at Leith, Immingham and Sheerness.

Figure-4 shows the absolute errors in the phase of the modelled M2 constituent. The model performs well using all three boundary forcing datasets, with values generally below  $10^\circ$ . Phase is good around some estuarine areas, e.g. the Severn Estuary and Liverpool Bay and Leith but worse at Immingham (Humber) and Sheerness (Thames). Phase errors at Port Ellen are notably bad, reaching almost  $80^\circ$  for the TPXO and FES cases and  $100^\circ$  for the NEA case (the figure colormaps are saturated at the top end). These large phase errors are likely due to extreme proximity to the regional amphidrome.

Figure-5 shows a direct comparison of M2 amplitude and phase errors from the FES and NEA cases against the control case (TPXO boundary forcing). M2 Amplitude errors in the FES case are virtually identical to the TPXO case, with differences on the order of a few cm. However, for the NEA case, errors are larger everywhere, significantly so on the East and Scottish coasts.

For phase, changes in accuracy are generally small for both the FES and NEA cases. For the FES case, errors along the East coast are on the order of  $5 - 10^\circ$  worse. Elsewhere, there is little difference for the FES case. For the NEA case, errors are worse by a similar magnitude on the west coast and slightly improved around the East Anglian coastline. Although these changes are small, many are consistent along their respective coastlines/in their respective regions and are therefore worthy of note. The largest decrease in accuracy is seen at Port Ellen (for the NEA case). Again, this is likely due to proximity to the nearby amphidrome.

A more general overview of six of the largest constituents is now presented. These constituents are M2, S2, K2, O1, K1, N2. For each constituent, two metrics are calculated over all 41 locations used: the mean error or bias (ME) and the root mean squared error (RMSE), which are calculated separately for amplitude and phase. These metrics are also compared against their counterparts for AMM7 and CS3X from [1]. These runs will henceforth be referred to as the FURNER model runs. It is important to note that the FURNER runs were calculated over a different time period and for model runs with a longer spinup.

Tables 3-5 show the mean error and RMSE for each of the six constituents and each model run. For all cases, including the FURNER runs, the models underestimate amplitudes for most constituents. Of the runs in this report, the NEA case generally performs worst, with the control and FES cases seeing a similar performance.

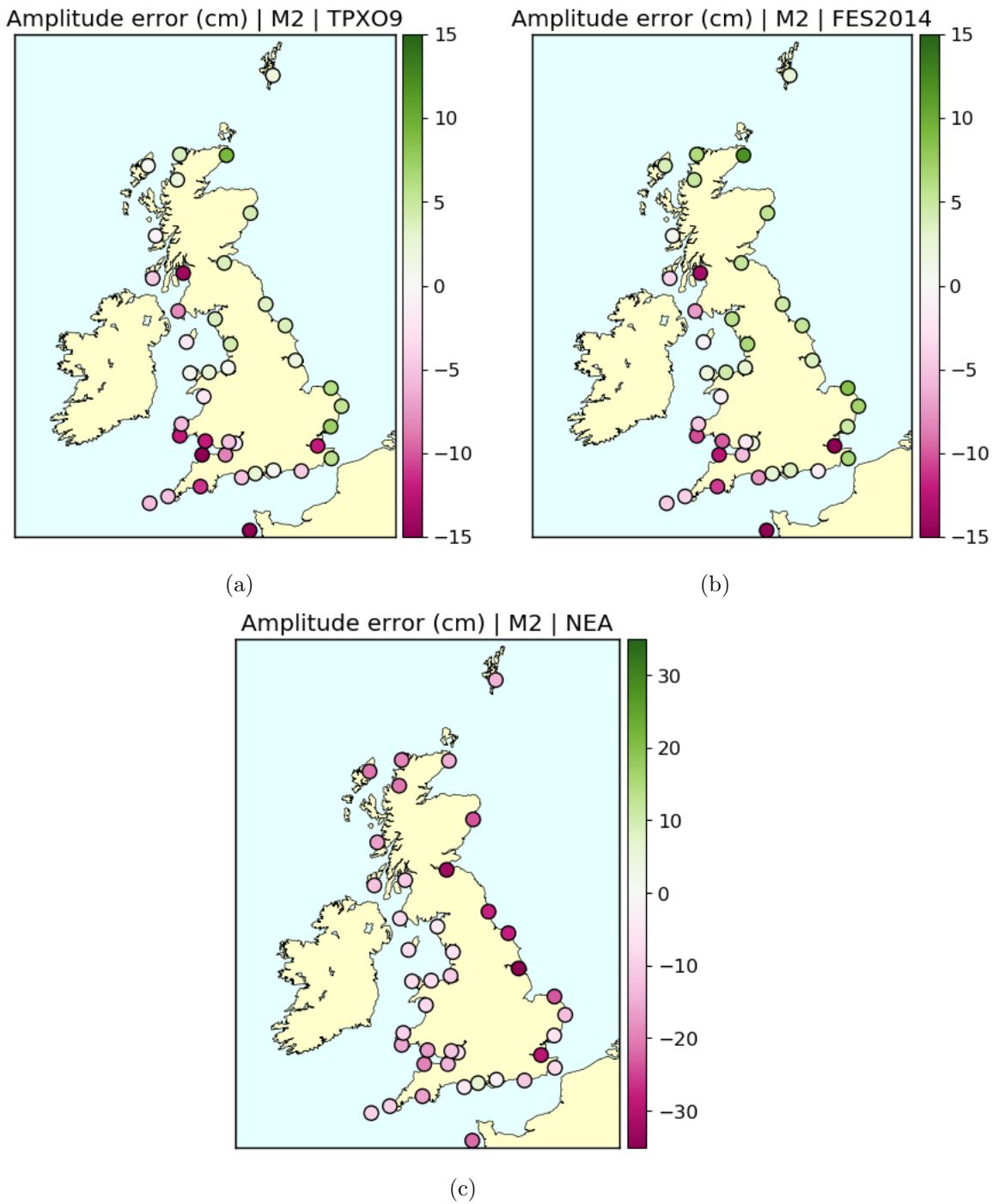
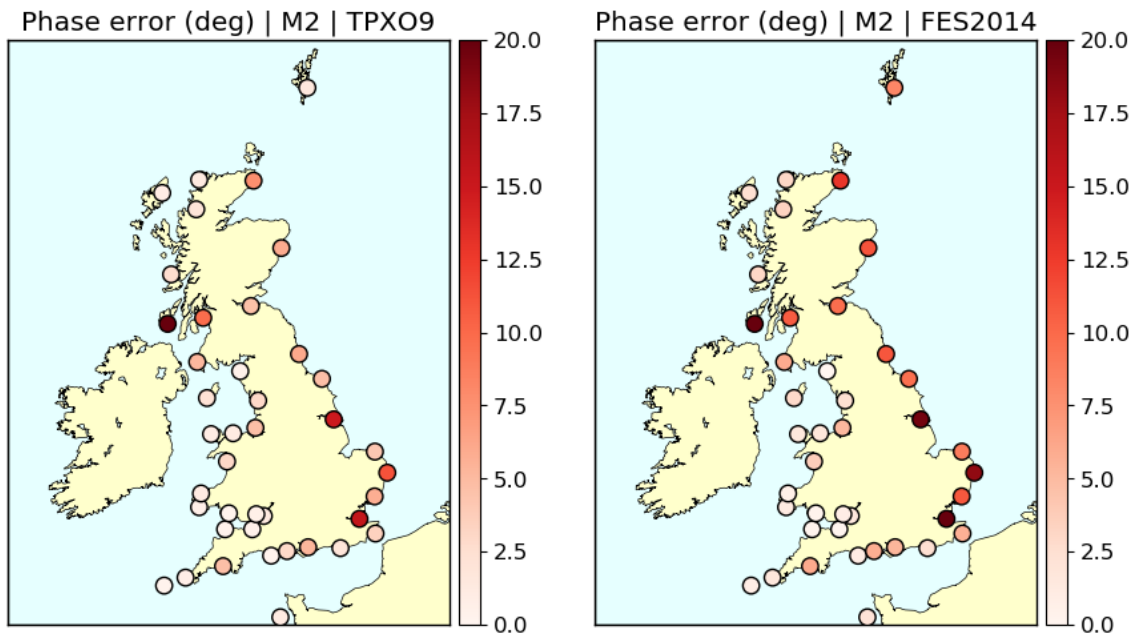
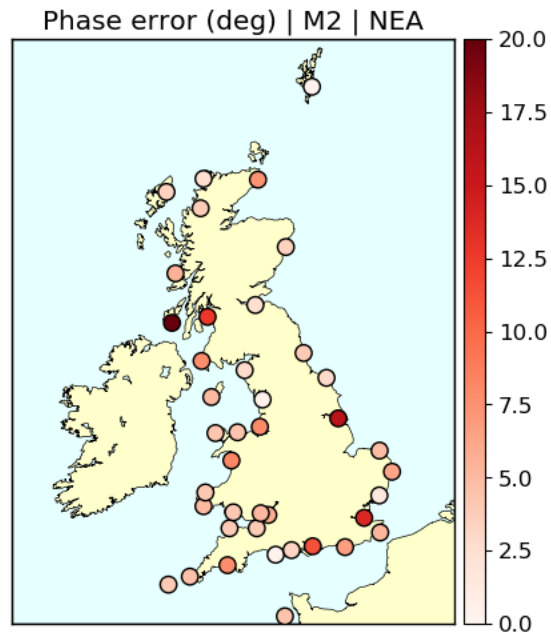


Figure 3: Errors in M2 amplitude for different tidal boundary datasets.



(a)

(b)



(c)

Figure 4: Absolute errors in M2 phase for different tidal boundary datasets. Note: Colormap is saturated at the top end for Port Ellen where it reaches  $80^\circ$  for the TPXO and FES cases and  $100^\circ$  for the NEA case.

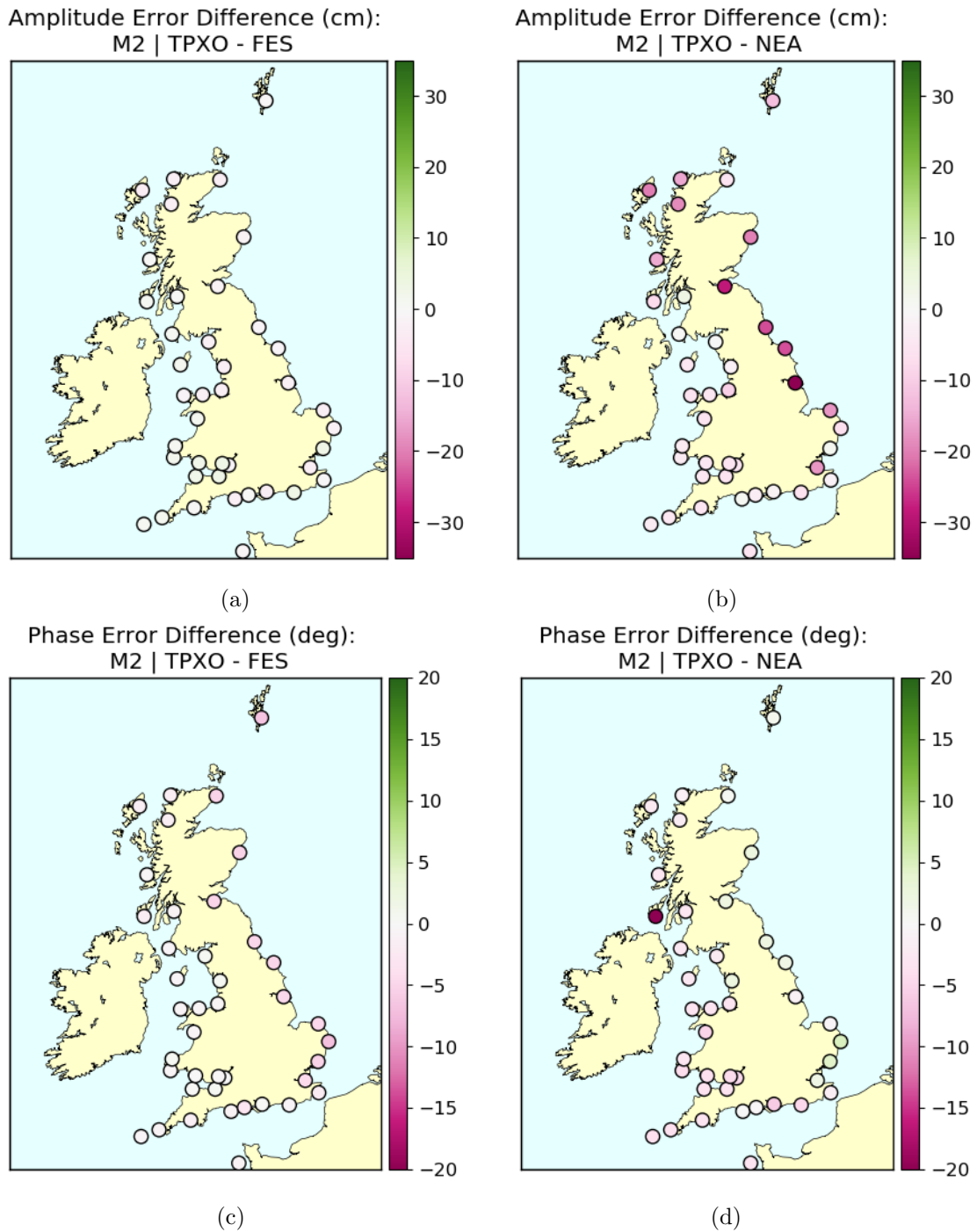


Figure 5: RMSE differences in M2 amplitude and phase error difference between models run with different tidal boundary forcing datasets. Positive means improvement relative to the control run (TPXO9).

| <b>Amplitude<br/>ME (cm)</b> | Ctrl | NEA  | FES  | AMM7  | CS3X |
|------------------------------|------|------|------|-------|------|
| M2                           | -2.8 | -14  | -0.5 | -10.5 | -5.9 |
| S2                           | 0.4  | -4.4 | -1.0 | -1.2  | -2   |
| K2                           | -0.9 | -2.7 | -1.1 | -0.4  | -1.1 |
| O1                           | -0.5 | -1.2 | -0.2 | -0.3  | -1.4 |
| K1                           | -0.3 | -1.9 | 4.1  | -0.4  | -0.5 |
| N2                           | -1.4 | -4.6 | -1.9 | -1.6  | -1.6 |

Table 3: Mean errors in amplitude for 6 constituents over 41 Class A UK tide gauge locations. Errors calculated for models run with three different tidal boundary conditions (TPX09, NEA and FES) with comparisons to AMM7 and CS3X.

| <b>Amplitude<br/>RMSE (cm)</b> | Ctrl | NEA  | FES | AMM7 | CS3X |
|--------------------------------|------|------|-----|------|------|
| M2                             | 6.9  | 16.6 | 7.1 | 14.5 | 16.7 |
| S2                             | 2.8  | 5.4  | 3.2 | 3.3  | 6.5  |
| K2                             | 1.4  | 3.0  | 1.4 | 1.4  | 2.5  |
| O1                             | 0.6  | 1.4  | 0.4 | 0.7  | 1.6  |
| K1                             | 0.9  | 2.1  | 4.9 | 1.1  | 1.0  |
| N2                             | 2.3  | 5.2  | 2.9 | 3.1  | 4.1  |

Table 4: RMSE in amplitude for 6 constituents over 41 Class A UK tide gauge locations. Errors calculated for models run with three different tidal boundary conditions (TPX09, NEA and FES) with comparisons to AMM7 and CS3X.

| <b>Phase<br/>RMSE (deg)</b> | Ctrl | NEA  | FES  | AMM7 | CS3X |
|-----------------------------|------|------|------|------|------|
| M2                          | 13.3 | 17.0 | 14.6 | 10.3 | 12.5 |
| S2                          | 7.4  | 10.1 | 9.4  | 7.7  | 9.4  |
| K2                          | 8.0  | 11.8 | 7.6  | 9.1  | 10.5 |
| O1                          | 2.8  | 5.6  | 3.5  | 7.9  | 17.0 |
| K1                          | 8.8  | 8.1  | 26.5 | 10.4 | 9.9  |
| N2                          | 14.0 | 20.1 | 15.7 | 14.8 | 15.3 |

Table 5: Absolute errors in phase for 6 constituents over 41 Class A UK tide gauge locations. Errors calculated for models run with three different tidal boundary conditions (TPX09, NEA and FES) with comparisons to AMM7 and CS3X.



### 4.2.2 Tidal Range and High Water Lag

Some class A locations are omitted due to poor data quality or large gaps for the year 2014, e.g. Port Ellen and Bournemouth.

Figure-6 shows the mean error in tidal range around the UK for each tidal dataset case over the year 2014. The spatial structure of these errors is broadly similar to those seen for M2 amplitude in the previous section. For the control and FES cases, the range is underestimated in and around the Severn Estuary, Strait of Moyle and the English Channel. For the NEA case, tidal ranges are underestimate universally, especially along the East coast of the UK.

Figure-7 shows the mean lag in high water around the UK for each tidal dataset for the year 2014. In all three cases, the high water arrives late for most locations, with the notable exception of Immingham. This universal late arrival of high water might suggest a bottom friction coefficient that is too high. This is discussed more in Section-.

Figure-8 shows a comparison between the control and FES/NEA cases of tidal range RMSE and HW lag. For the NEA case, significant decreases in the accuracy of tidal range can be seen along the East coast and northern Scotland. For the FES case, differences are small and insignificant. Use of the NEA dataset sees widespread improvement (over TPXO) in high water lag RMSE, most notably at portsmouth and along the west coast. The use of FES also sees some improvements, especially along the east coast.

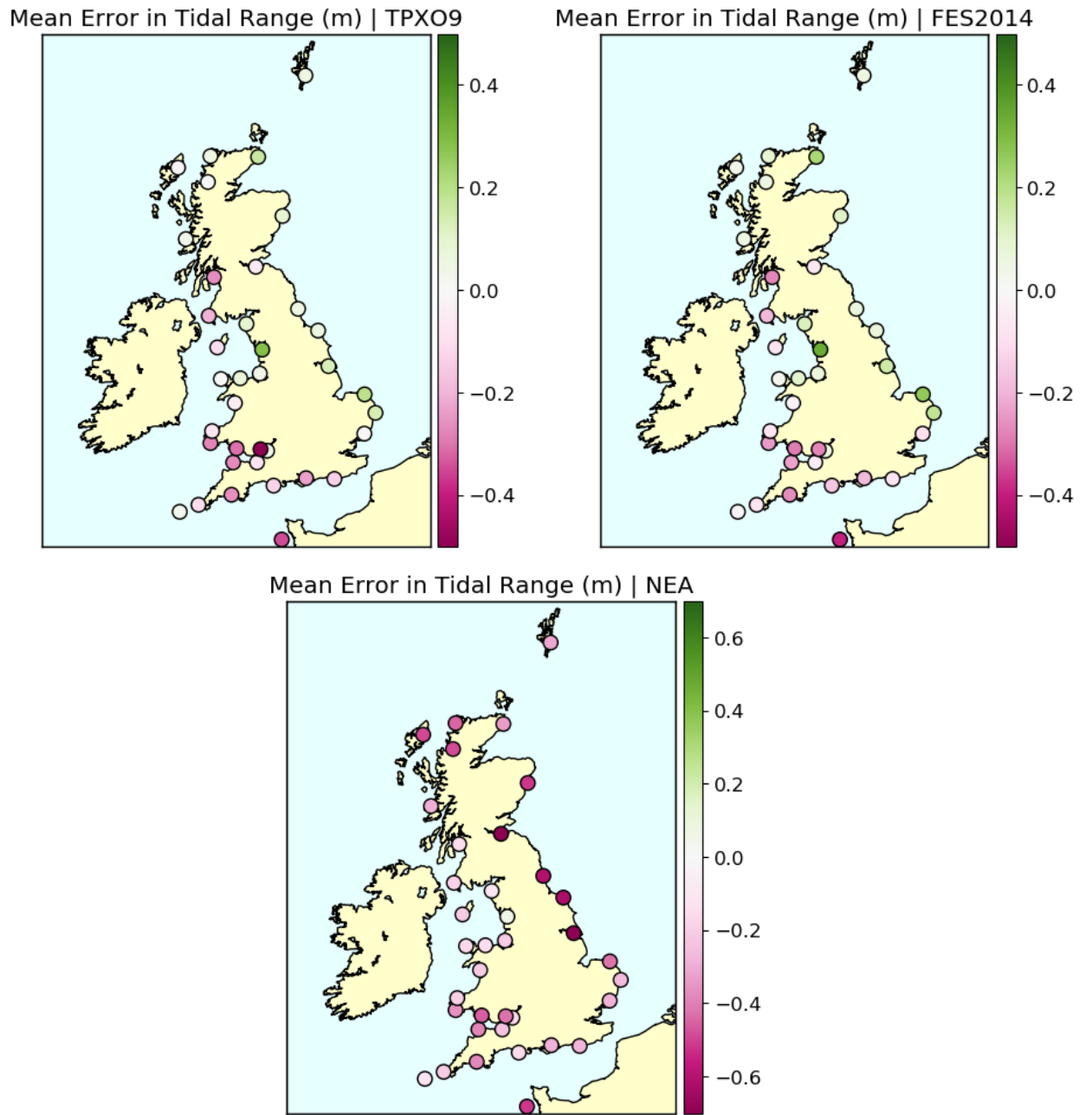


Figure 6: Mean errors in tidal range over 2014. Tidal range for each tidal cycle calculated as the difference between maximum and minimum value. Errors calculated for each tidal cycle are then averaged. Positive means overestimation by model.

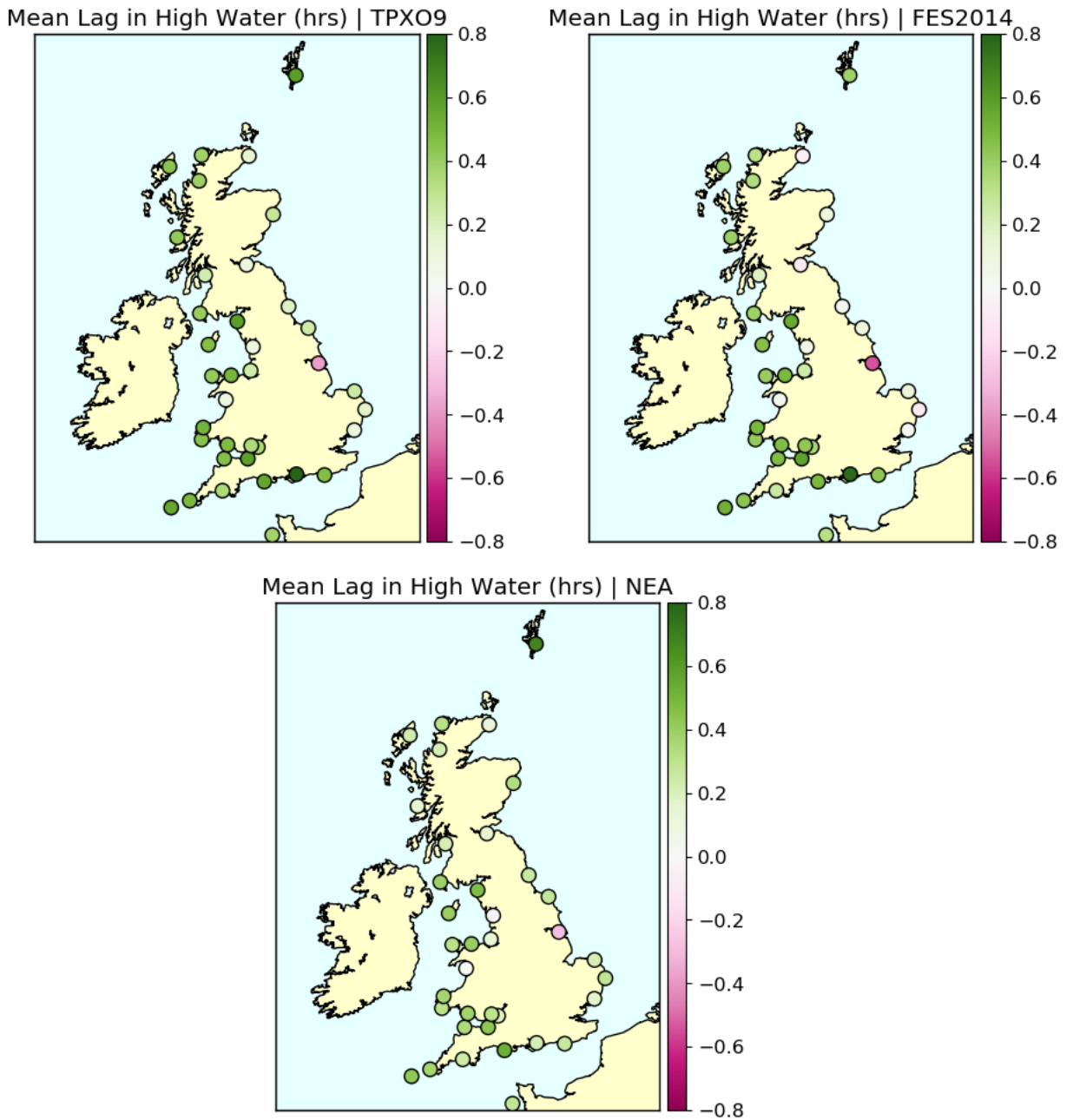


Figure 7: Mean model errors in high water lag over 2014. Tidal range for each tidal cycle calculated as the difference between maximum and minimum value. Errors calculated for each tidal cycle are then averaged. Positive means model HW was late.

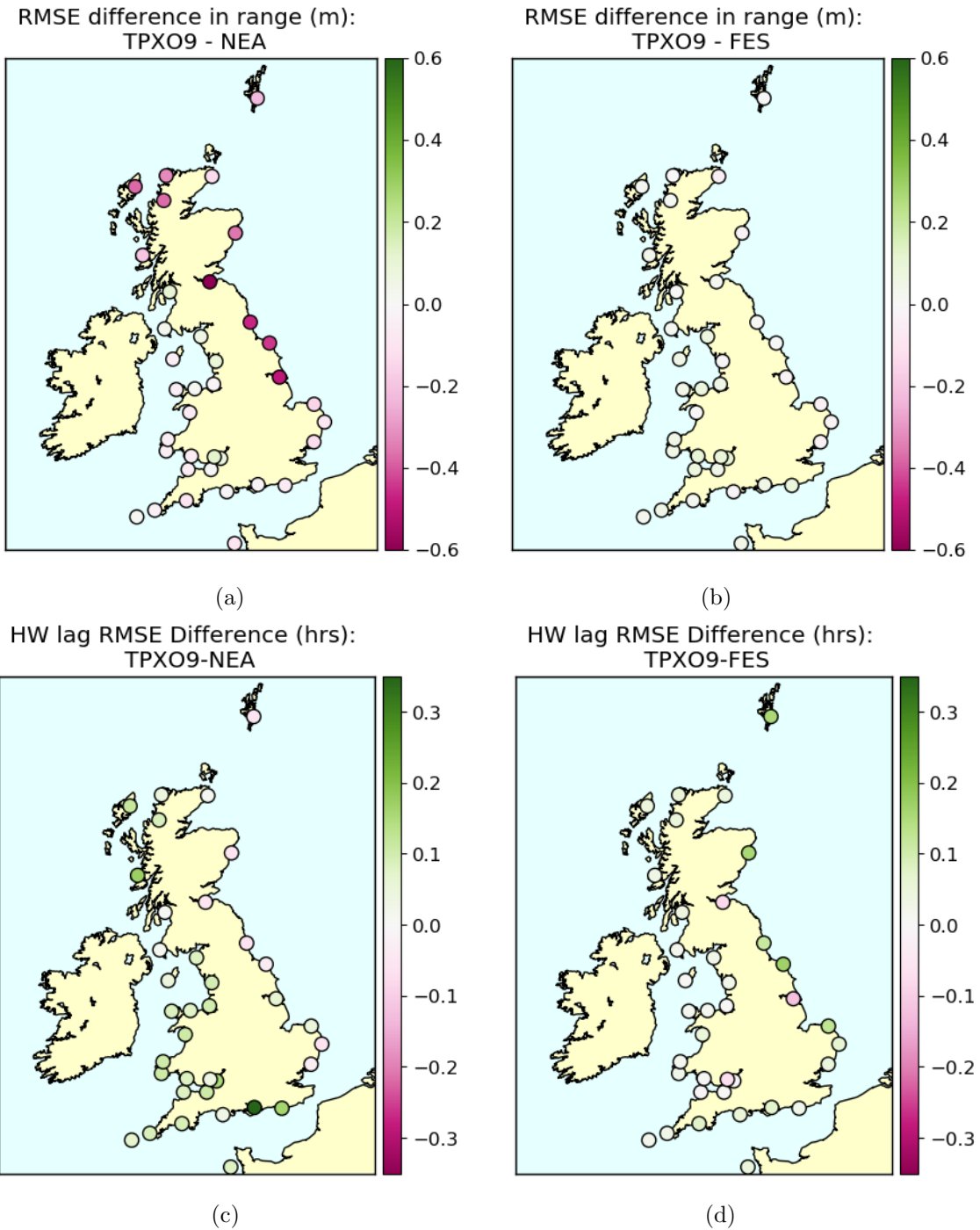


Figure 8: Differences in RMSE of range (a-b) and HW lag (c-d) between models run with NEA/FES boundary conditions and TPX09 (control). Positive means improvement relative to TPX09.

### 4.3 Varying the Bottom Friction Coefficient

In this section the results of the BF class of experiments are shown. These are three separate experiments where the bottom friction coefficient  $C_B$  is reduced compared to the control run.

#### 4.3.1 Amplitude and Phase

Figure-9 shows the M2 amplitude error for the three BF experiments and the control. There are some notable areas where the mean error changes sign for the BF experiments: top of the Severn Estuary and Sheerness. In these areas, the universal reduction of  $C_B$  has resulted in the model now overestimating the amplitude of M2, whereas it was previously underestimated. Both areas consist of complex coastal geometry, shallow water and resonant effects. Elsewhere the spatial structure is broadly similar to the control run.

Figure-10 shows the M2 phase error for the three BF experiments and the control. The spatial structure is similar for all runs. There is still a large outlier at Port Ellen, so the errors likely caused by the nearby amphidrome are not removed. Estuarine areas on the east coast still perform poorly, however those on the west are better.

Figure-11 shows the difference in the absolute amplitude error between the three BF runs and the control run. Each reduction results in larger differences from the control. There are some improvements: the Cornich coast, some of the Severn Estuary and Sheerness. However, there are more, larger decreases in the accuracy of the model M2 amplitude elsewhere.

Figure-12 shows the difference in phase error between the three BF runs and the control. For the north of the UK, differences are small for all three model runs (except at Port Ellen for BF18). The south sees decreases in accuracy in the south, especially in the English Channel and Severn Estuary. The model errors increase in magnitude for these areas as bottom friction is reduced.

Tables 6-8 shows statistics over all locations for six tidal constituents for the BF experiments, control and the AMM7/CS3X runs in [3]. For M2 and S2, RMSE increases as  $C_B$  decreases, however all runs are still generally better than AMM7 and CS3X. For the smaller constituents the RMSE story is more mixed, although all values are of a similar order to AMM7 and CS3X. The general trend in phase RMSE for the six constituents studied is also to increase as bottom friction decreases.

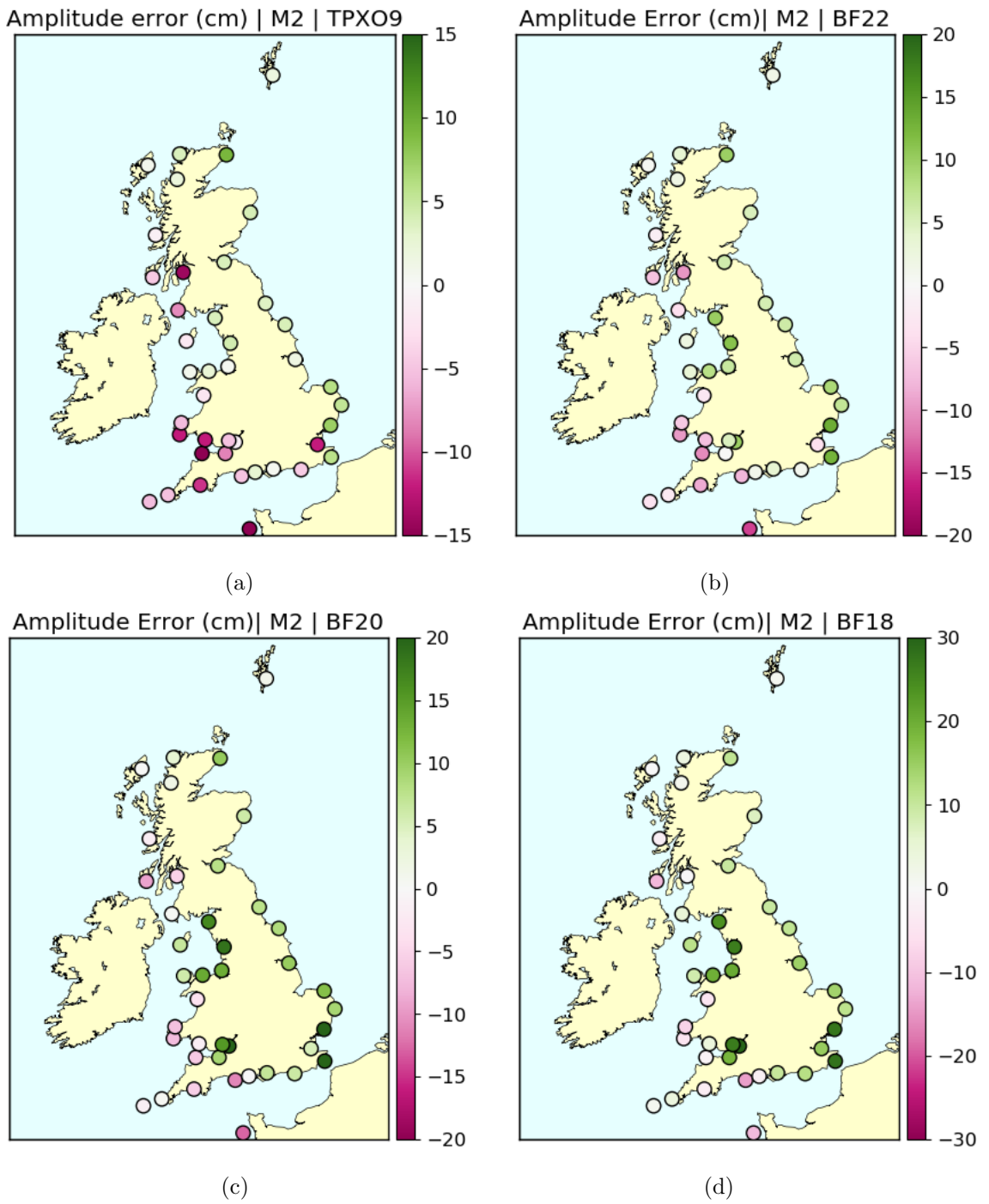


Figure 9: Errors in M2 amplitude for the CTRL run and different model runs with varying bottom friction.

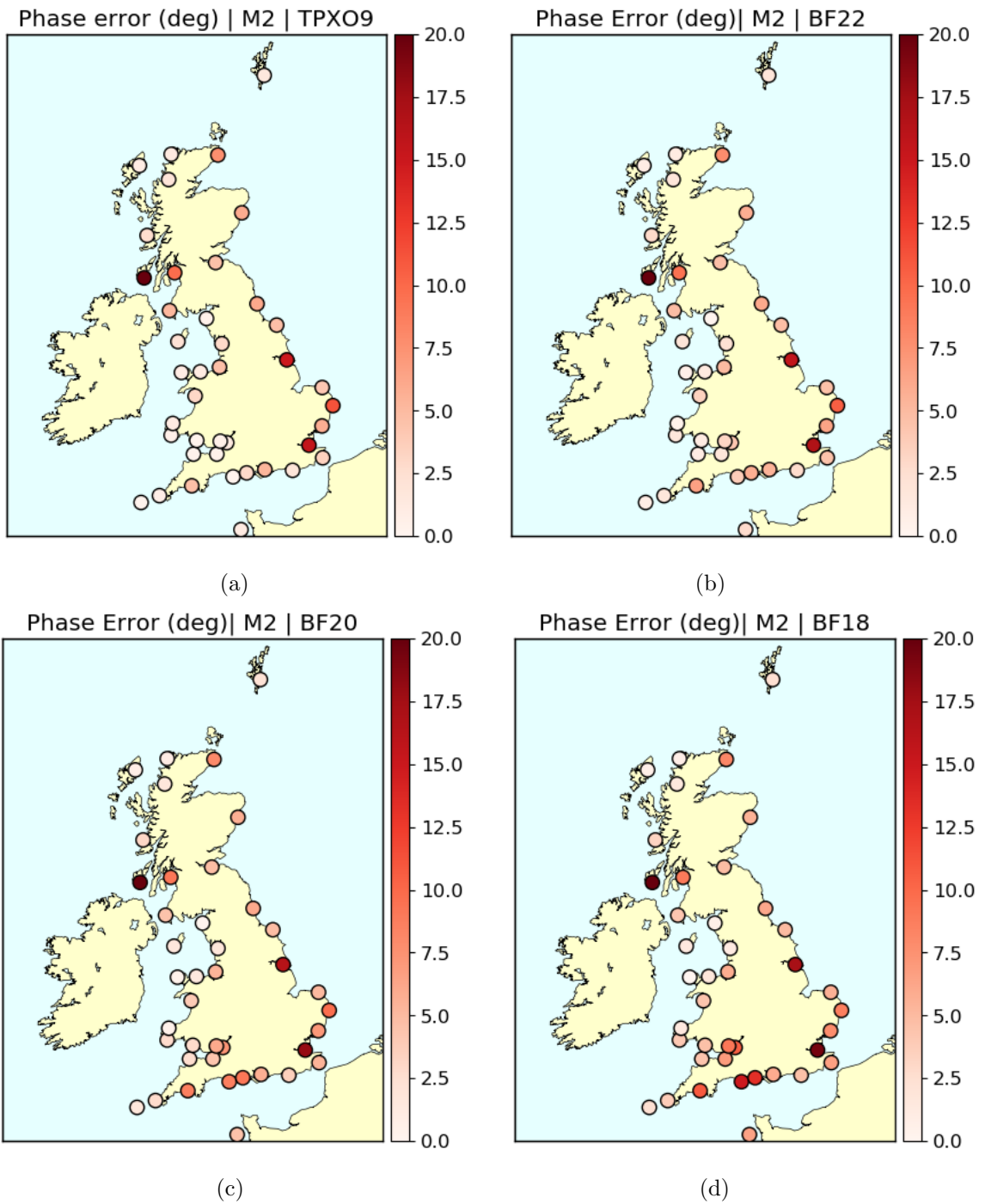


Figure 10: Absolute errors in M2 phase for different values of the bottom friction parameter. Note: Colormap is saturated at the top end for Port Ellen.

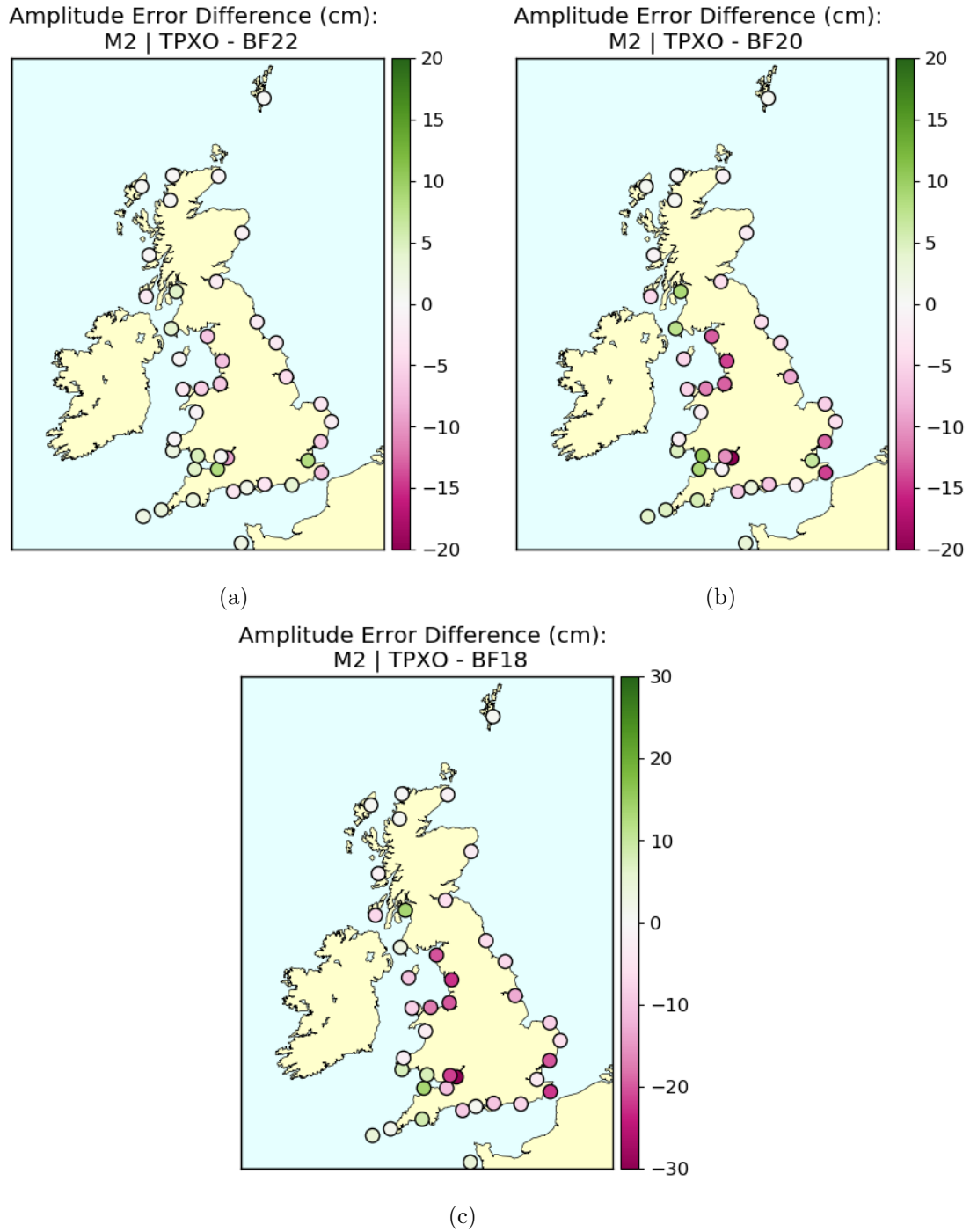


Figure 11: RMSE differences in M2 amplitude between models runs with varying values of the bottom friction parameter. Positive means improvement relative to the control run.



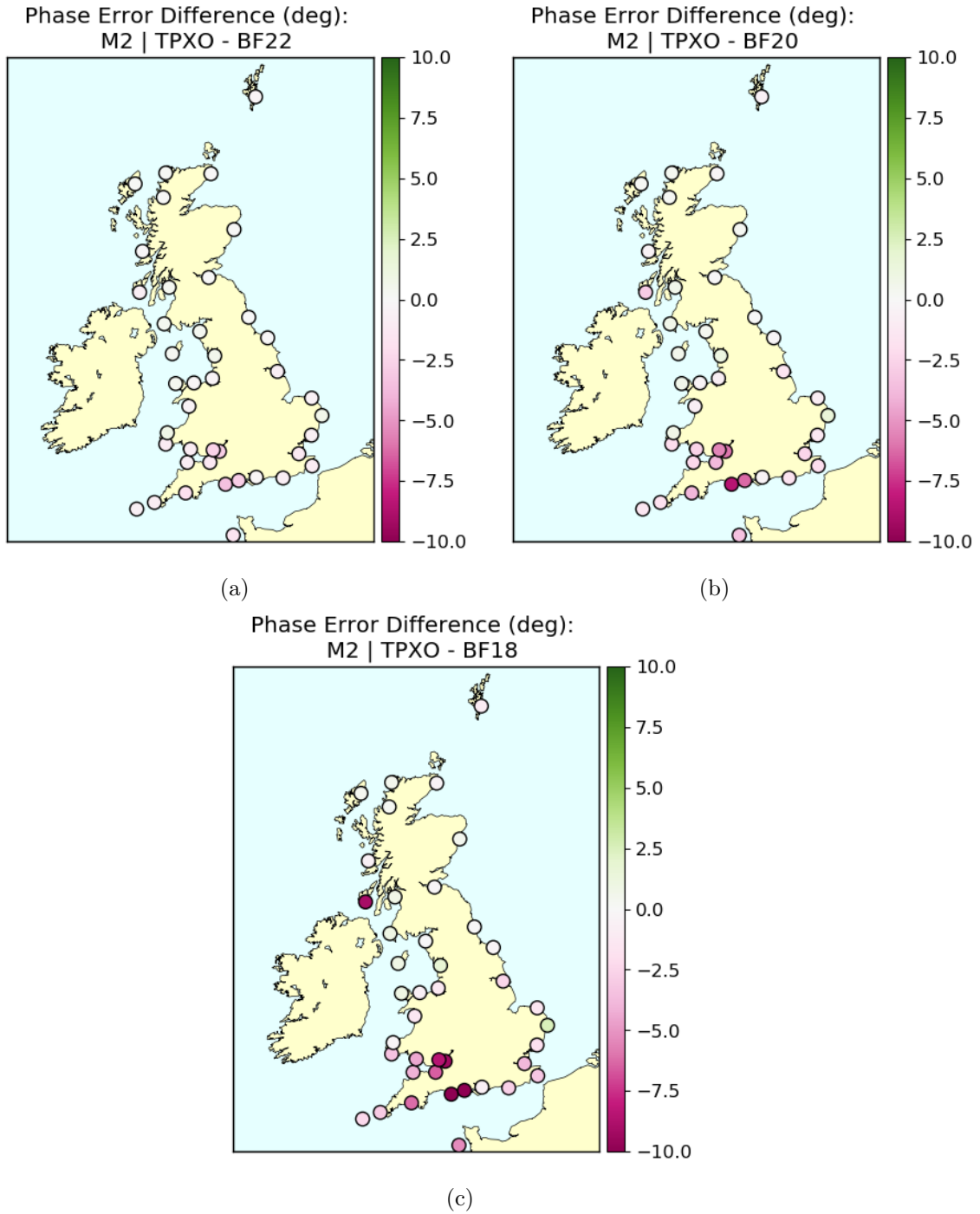


Figure 12: Difference in M2 phase error between models runs with varying values of the bottom friction parameter. Positive means improvement relative to the control run.

| <b>Amplitude<br/>ME (cm)</b> | Ctrl | BF22 | BF20 | BF18 | AMM7  | CS3X |
|------------------------------|------|------|------|------|-------|------|
| M2                           | -2.8 | 1.3  | 4.5  | 8.0  | -10.5 | -5.9 |
| S2                           | 0.4  | 1.9  | 3.6  | 5.5  | -1.2  | -2.0 |
| K2                           | -0.9 | -0.4 | -0.0 | 0.5  | -0.4  | -1.1 |
| O1                           | -0.5 | -0.3 | -0.2 | -0.0 | -0.3  | -1.4 |
| K1                           | -0.3 | -0.1 | 0.1  | 0.3  | -0.4  | -0.5 |
| N2                           | -1.4 | -0.7 | -0.1 | 0.7  | -1.6  | -1.6 |

Table 6: Mean errors in amplitude for 6 constituents over 41 Class A UK tide gauge locations. Errors calculated for model runs with varying values for the bottom friction parameter  $C_B$ , with comparisons to AMM7 and CS3X.

| <b>Amplitude<br/>RMSE (cm)</b> | Ctrl | BF22 | BF20 | BF18 | AMM7 | CS3X |
|--------------------------------|------|------|------|------|------|------|
| M2                             | 6.9  | 7.1  | 10.0 | 14.2 | 14.5 | 16.7 |
| S2                             | 2.8  | 3.9  | 5.8  | 8.2  | 3.3  | 6.5  |
| K2                             | 1.4  | 1.0  | 0.9  | 1.4  | 1.4  | 2.5  |
| O1                             | 0.6  | 0.5  | 0.4  | 0.5  | 0.7  | 1.6  |
| K1                             | 0.9  | 0.9  | 1.0  | 1.1  | 1.1  | 1.0  |
| N2                             | 2.3  | 1.6  | 1.4  | 1.8  | 3.1  | 4.1  |

Table 7: RMSE in amplitude for 6 constituents over 41 Class A UK tide gauge locations. Errors calculated for varying values for the bottom friction parameter  $C_B$ , with comparisons to AMM7 and CS3X.

| <b>Phase<br/>RMSE (deg)</b> | Ctrl | BF22 | BF20 | BF18 | AMM7 | CS3X |
|-----------------------------|------|------|------|------|------|------|
| M2                          | 13.3 | 13.5 | 14.1 | 15.5 | 10.3 | 12.5 |
| S2                          | 7.4  | 7.4  | 7.7  | 8.2  | 7.7  | 9.4  |
| K2                          | 8.0  | 7.8  | 7.8  | 8.1  | 9.1  | 10.5 |
| O1                          | 2.8  | 5.8  | 9.6  | 13.6 | 7.9  | 17.0 |
| K1                          | 8.8  | 8.9  | 9.1  | 9.3  | 10.4 | 9.9  |
| N2                          | 14.0 | 14.1 | 14.5 | 15.2 | 14.8 | 15.3 |

Table 8: Absolute errors in phase for 6 constituents over 41 Class A UK tide gauge locations. Errors calculated for varying values for the bottom friction parameter  $C_B$ , with comparisons to AMM7 and CS3X.

### 4.3.2 Tidal Range and High Water Lag

Figure-13 shows the mean error in tidal range for the three BF runs and control run. As the bottom friction coefficient is decreased, the mean error increases with some locations seeing a change in sign. When the bottom friction coefficient reaches 0.0018, most locations overestimate the tidal range, even in the Severn Estuary where it was previously underestimated by a relatively large amount.

Figure-14 shows the mean lag in the high water for the three BF runs and control run. For all runs, high waters arrive late at most locations, with the exception of Immingham. Portsmouth is also notably bad for all runs.

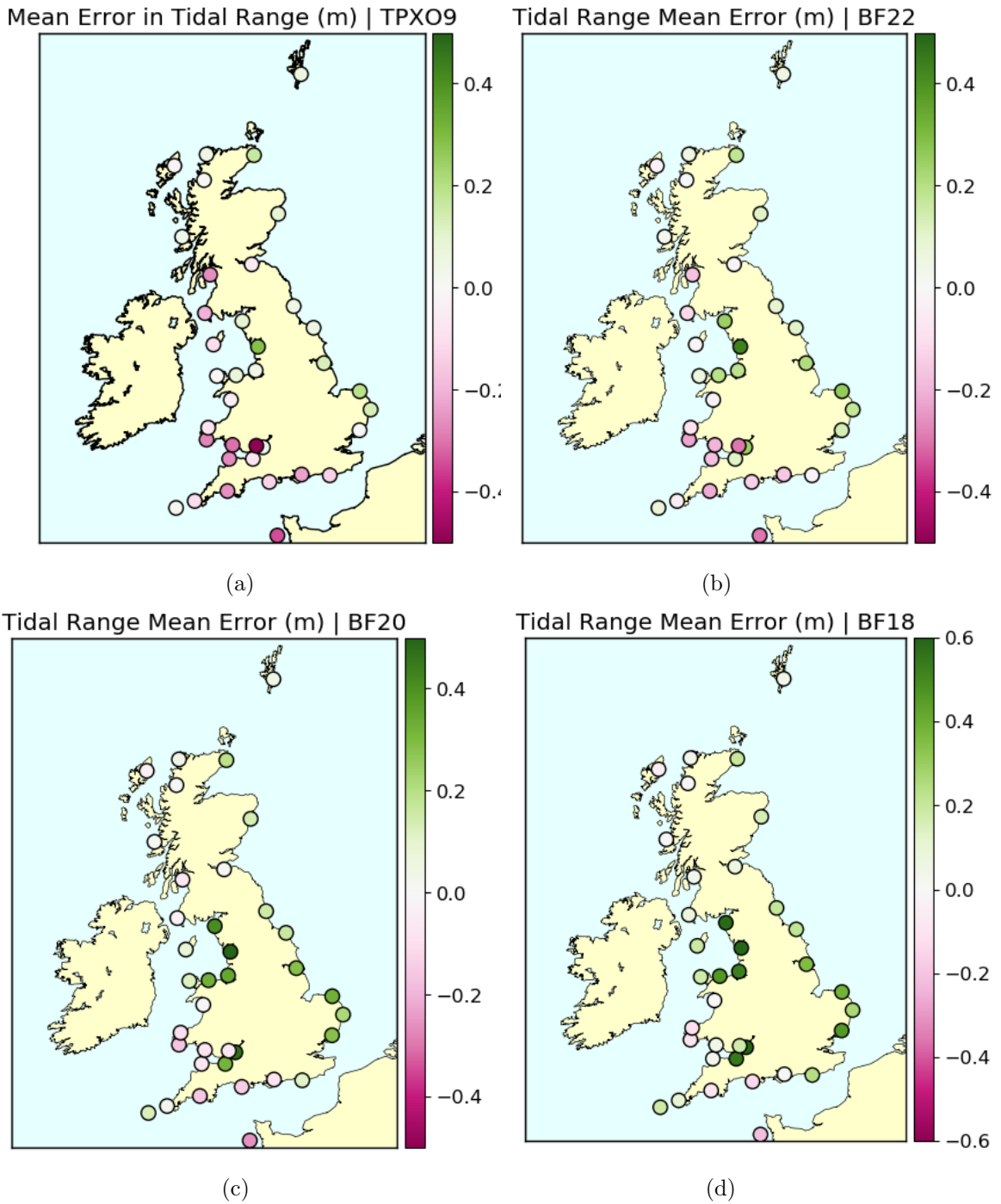


Figure 13: Mean errors in tidal range over 2014 for different values of bottom friction parameter  $C_B$ . Tidal range for each tidal cycle calculated as the difference between maximum and minimum value. Errors calculated for each tidal cycle are then averaged. Positive means overestimation by model.

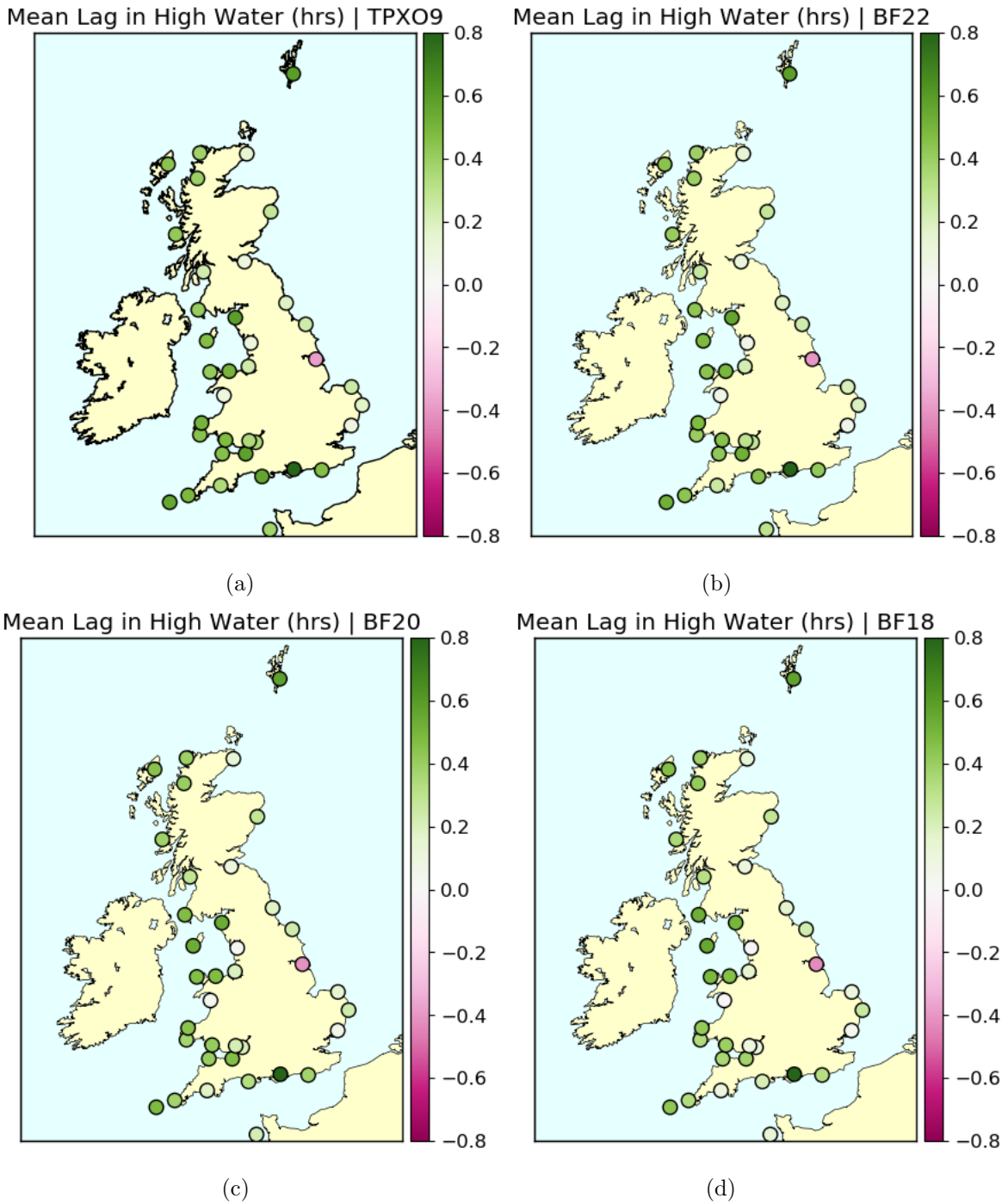


Figure 14: Mean model errors in high water lag over 2014 for different values of bottom friction parameter  $C_B$ . Tidal range for each tidal cycle calculated as the difference between maximum and minimum value. Errors calculated for each tidal cycle are then averaged. Positive means model HW was late.

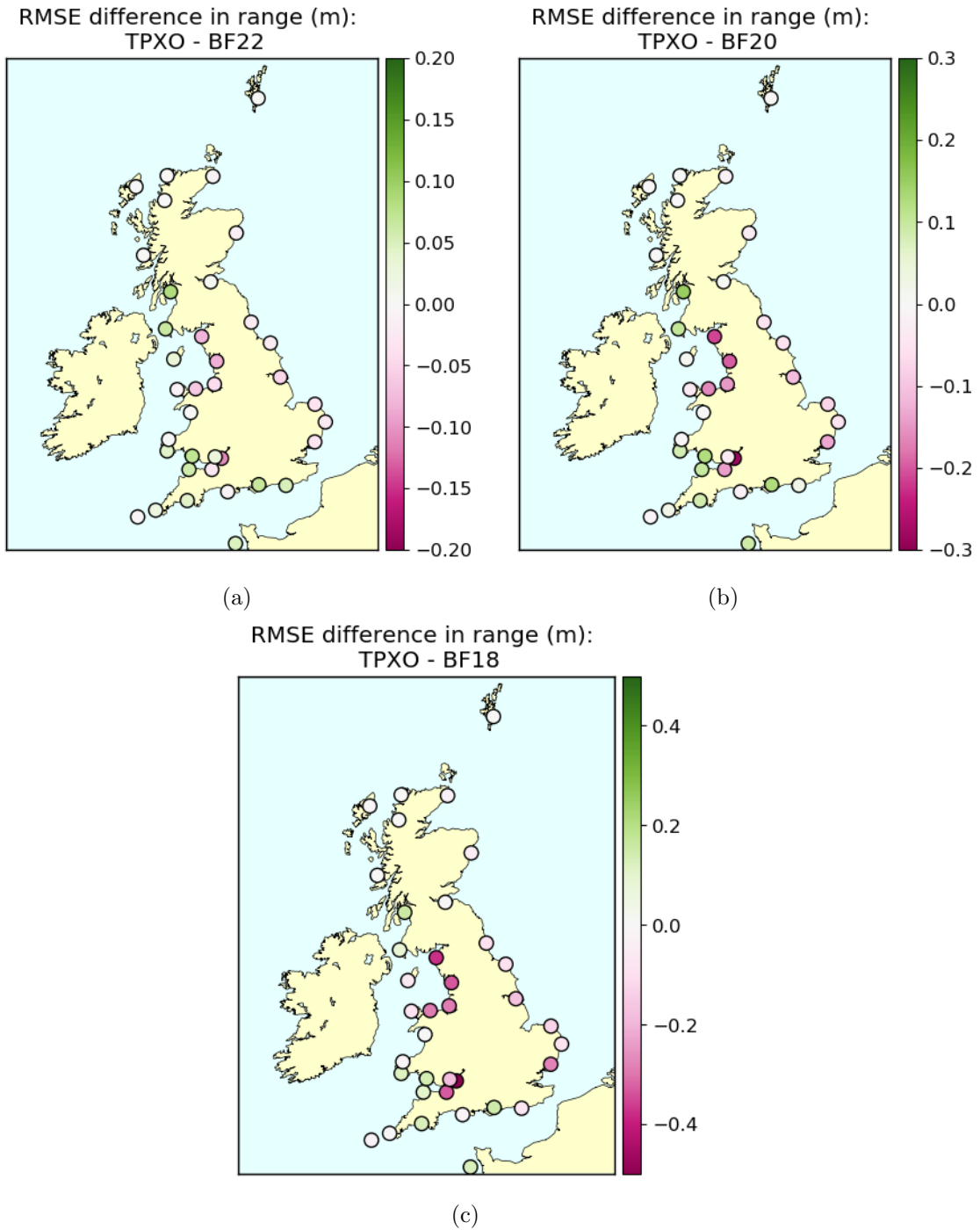


Figure 15: Differences in RMSE of range between the control run (TPXO) and models run varying values of bottom friction parameter  $C_B$ . Positive means improvement relative to TPXO9.

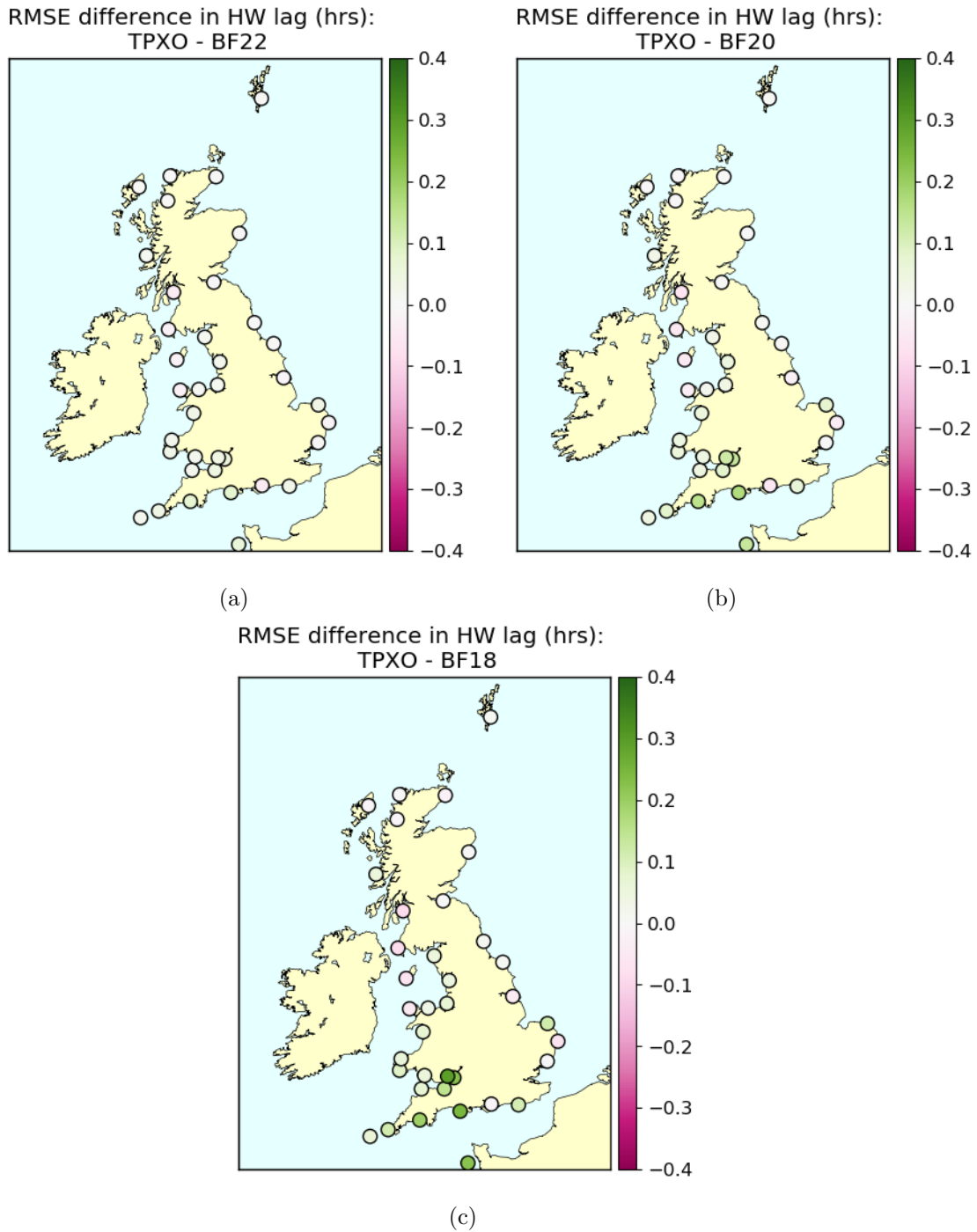


Figure 16: Differences in RMSE of high water lag between the control run (TPXO) and models run varying values of bottom friction parameter  $C_B$ . Positive means improvement relative to TPXO9.

## 5 Summary and Recommendations

1. The work presented in this report is an investigation into the impact of varying tidal boundary conditions and bottom friction has for the skill of an AMM15 configuration of the NEMO ocean model.
2. Three numerical experiments are run with variable tidal forcing at the domain boundaries. Variable numbers of harmonic constituents from three datasets are used independently in each experiment: 15 from TPXO9, 26 from NEA and 31 from FES2014. The bottom friction coefficient is fixed at  $C_B = 0.0024$ .
3. Four experiments are run with variable bottom friction parameters. The values investigated are  $C_B = 0.0024$ , 0.0022, 0.0020 and 0.0018.
4. The model run using 15 constituents from the TPXO9 dataset and  $C_B = 0.0024$  is named as the control run.
5. Model skill is evaluated using a comparison of model and observed harmonic amplitudes and phases at 41 UK locations (Class A ports). A comparison of mean tidal range errors and lag time in the timing of high waters is also made.
6. A comparison is also made to previous work with an AMM7 configuration and CS3X output. The increased resolution of AMM15 compared to AMM7 was shown to reduce both amplitude and phase errors at most UK locations.
7. **Results of variable tidal forcing experiments:** Across six of the largest constituents, the FES2014 and TPXO9 datasets perform well across all locations, for both amplitude and phase. Broadly speaking, both datasets give comparable results. For M2 amplitude, RMSE for FES2014 and TPXO9 datasets is approximately half that of NEA, which has errors of comparable magnitude to AMM7 and CS3X. Mean errors in tidal range are smaller when using TPXO9 or FES2014 over NEA. Notably, NEA generally performs better than either when inspecting the timing of high waters.
8. **Results of variable bottom friction coefficient experiments:** Across six constituents, RMSE at all locations increases as bottom friction decreases. Despite this, the AMM15 configuration still performs similarly or better than AMM7 and CS3X for the three highest bottom friction coefficients. Phase RMSE does not change significantly when varying  $C_B$  and is broadly comparable to that seen for AMM7 and CS3X. Tidal range RMSE also increases as  $C_B$  decreases, however RMSE in the timing of high water decreases at most locations, especially in southwestern areas.
9. **Recommendations:** Based on these results, the recommended configuration for AMM15 NEMO-surge is to use either the FES2014 or TPXO9 datasets for lateral boundary conditions and a value of  $C_B = 0.0024$  for the bottom friction parameterization. Additionally, if the computing resources are available, AMM15 should be used for improved model output when compared to AMM7.



## References

- [1] J. A. Graham, E. O’Dea, J. Holt, J. Polton, H. T. Hewitt, R. Furner, K. Guihou, A. Brereton, A. Arnold, S. Wakelin, J. M. C. Sanchez, C. G. M. Adame *AMM15: a new high-resolution NEMO configuration for operational simulation of the European north-west shelf* 2018: Geosci. Model Dev.
- [2] G. Madec, P. Delecluse, M. Imbard, C. Levy *OPA 8 Ocean General Circulation Model - Reference Manual*, Technical Report, LODYC/IPSL Note 11, 1998
- [3] R. Furner, J Williams, K Horsburgh, A Saulter, *AMM7: Setting up an accurate tidal model*, Forecasting Research, Technical Report No: 610, 2016
- [4] <https://www.aviso.altimetry.fr/en/data/products/auxiliary-products/references.html>
- [5] Carrere L., F. Lyard, M. Cancet, A. Guillot, N. Picot: FES 2014, a new tidal model - Validation results and perspectives for improvements, presentation to ESA Living Planet Conference, Prague 2016.
- [6] Flowerdew, J., Horsburgh, K., Wilson, C., and Mylne, K. (2010), Development and evaluation of an ensemble forecasting system for coastal storm surges, *Quarterly Journal of the Royal Meteorological Society*, 136(651), 1444–1456, DOI: 10.1002/qj.648.
- [7] Horsburgh, K. J., Williams, J. A., Flowerdew, J., Mylne, K. (2008) Aspects of operational model predictive skill during an extreme storm surge event. *Journal of Flood Risk Management*, 1, 213-221.
- [8] Madec, G., et al (2014), NEMO reference manual v3.6, Tech. Rep. 27 ISSN 1288–1619, Note du Pole de modelisation, Institut Pierre-Simon Laplace (IPSL).